Analyst

PAPER

View Article Online
View Journal | View Issue

Cite this: *Analyst*, 2025, **150**, 4201

Assessment of IgG stability in a low pH elution buffer using ATR-FTIR spectroscopic imaging and microfluidics

Céline van Haaren, [a] Bernadette Byrne *[b] and Sergei G. Kazarian *[a]

Monoclonal antibodies (mAbs) represent the largest class of biopharmaceuticals, playing a vital role in the treatment of a wide range of diseases. Although the production of high quality mAbs has significantly improved over the last three decades, particularly in terms of scale and yield, the antibody's complex nature poses several challenges during bioprocessing. One of the main challenges in the production of mAbs is the formation of aggregates, which may cause harmful immunogenic responses in patients if not removed from the final drug product. Exposure to a low pH environment during protein A chromatography and viral inactivation is thought to be the major contributor to aggregate formation and has therefore been a topic of study for many years. Here, we investigate the stability of an IgG4 mAb in a low pH elution buffer (pH 3.5) under flow using ATR-FTIR spectroscopic imaging. This method, making use of a microfluidic set-up, enables non-destructive monitoring of mAb structural stability under bioprocessing-relevant conditions. Samples were (i) prepared through dialysis into the elution buffer and (ii) collected directly after elution from the protein A column, after which their stability was assessed under flow at two different temperatures (30 °C and 45 °C). Spectroscopic images and associated IR absorption spectra revealed that in both cases the protein in the low pH buffer underwent small, but measurable, structural changes at 30 °C. However, at 45 °C, the protein rapidly aggregated as indicated by a major shift in the Amide I peak position from 1637 cm^{-1} to 1625 cm^{-1}, representing formation of inter-molecular beta sheets. These results confirm the destabilising effect of the low pH environment and demonstrate the applicability of ATR-FTIR spectroscopic imaging in combination with microfluidics as a powerful analytical tool for the analysis of protein structural stability under flow.

Received 20th June 2025,
Accepted 1st August 2025

DOI: 10.1039/d5an00664c

rsc.li/analyst

1. Introduction

Monoclonal antibody (mAb) therapeutics remain the leading class of biopharmaceuticals, in terms of both approvals and sales, with immunoglobulin G (IgG) being the predominant mAb.[1] Due to the high specificity and affinity for their biological target, mAb-based therapeutics have proved to be successful in treating a range of diseases, including many cancers and infectious, respiratory and autoimmune diseases.[2] MAbs are typically produced in a large-scale process involving upstream mammalian cell culture and downstream purification, formulation and fill and finish steps.[3] Over the past 30 years, significant progress has been made towards the development of high yield and large-scale bioprocesses of therapeutic mAb products; however, one of the main challenges during the production of these mAbs remains aggregate formation.[4–6] Aggregate formation occurs when mAb molecules self-associate, leading to the formation of dimers, oligomers and ultimately larger particles. Typically, aggregation involves some degree of conformational or chemical change at the monomer level, which can be reversible or irreversible.[5,7] During bioprocessing, the physical and chemical stability of mAb molecules is strongly affected by the conditions the mAbs are exposed to. For example, mechanical and interfacial stresses caused by mixing, pumping and aeration of the cell culture can result in protein unfolding, and changes in pH and ionic strength during downstream purification steps may give rise to chemical instability.[8] Since aggregates in the final drug product may induce undesirable immunogenic responses in patients, the formation of aggregates needs to be prevented throughout bioprocessing, transport and storage.[9]

Research into aggregate formation is extensive; however, since aggregate formation is highly dependent on the protein in question and the environmental conditions it is exposed to, a full understanding of aggregation under the

[a]*Department of Chemical Engineering, Imperial College London, South Kensington Campus, London, SW7 2AZ, UK. E-mail: s.kazarian@imperial.ac.uk*
[b]*Department of Life Sciences, Imperial College London, South Kensington Campus, London, SW7 2AZ, UK. E-mail: b.byrne@imperial.ac.uk*

complex combination of stress conditions present during bioprocessing is lacking.[7] One key step in the downstream process thought to generate significant amounts of mAb aggregates is the low pH elution step during protein A chromatography.[10,11] Protein A chromatography is the so-called "capture" step, where mAbs are highly selectively bound to protein A resin at neutral pH as a result of the formation of hydrogen bonds, salt bridges and hydrophobic interactions, while impurities flow through the column.[12] After a simple wash step, the mAbs are eluted from the column using a low pH elution buffer, commonly a citrate, glycine or acetate buffer at pH 2.5–4.0.[10,13] This change from neutral pH to low pH is needed to release the tightly bound mAbs from the protein A resin, through electrostatic repulsion between histidine residues of protein A and the mAbs.[14] This type of affinity chromatography produces large quantities of highly pure protein and is used in virtually all large-scale mAb purification processes. However, the downsides of this step are the high costs of the protein A resin and the reportedly high propensity for aggregates to form due to low pH effects on protein stability.[10,15] In addition, the eluate is often subjected to a viral inactivation step, which comprises a low pH hold for up to several hours following protein A chromatography.[16] When IgG is exposed to a low pH environment, the charge distribution on the protein changes significantly, affecting its conformational and colloidal stability.[16] For example, ionizable side chains of the histidine, glutamic acid and aspartic acid residues can protonate, leaving the protein with a positive surface charge which affects inter-molecular interactions through electrostatic repulsion.[17] The colloidal stability, however, is also largely determined by the ionic strength of the solution, as both positive and negative ions can shield the mAb surface charge.[16] Furthermore, changes in intra-molecular electrostatic interactions resulting from the acidic environment may destabilize the native protein structure and lead to partial unfolding.[16,18]

Several studies have investigated the stability of IgG in strongly acidic buffers, with a focus on assessing the role of salts on aggregation kinetics[13,19,20] and/or evaluating the thermal stability of IgG at low pH.[13,20–22] In the context of bioprocessing, Mazzer *et al.* demonstrated that protein A chromatography results in significantly reduced IgG stability compared to exposure of IgG to the elution buffer on its own.[10,15] Their data suggested that the chromatography step accelerates aggregation considerably in the pH and concentration ranges tested (pH 2.78–3.11; 0.9–4.5 mg ml^{-1}), but that the mechanism of aggregation remains largely the same. This is likely due to the structural changes happening upon adsorption and desorption to the protein A column, which may expose areas of the protein involved in pH-dependent unfolding and subsequent aggregation.[10] Similarly, Gagnon *et al.* compared the stability of three IgG1 molecules with and without the protein A elution step and concluded that elution from the column resulted in a conformational variant of reduced size for all three proteins. Although elution did not directly cause aggregates to form, the protein was found to be more susceptible to aggregation as a result of secondary stress.[15] Furthermore, Wälchli *et al.* and Jin *et al.* studied mAb aggregation during the low pH viral inactivation process, focusing on various parameters including protein concentration, hold time and temperature, and the presence of additives.[16,17] Both studies found that under acidic conditions and at low ionic strength, the mAbs under study partially unfolded. Under these conditions, little change in molecular size or monomer content was observed, owing to the strong electrostatic repulsion between monomers. However, after neutralisation of the solution, the mAbs became prone to aggregation, resulting in an increase in molecular size and a decrease in monomer content.

In this study, we used ATR-FTIR spectroscopic imaging in combination with microfluidics to evaluate the structural stability of an IgG4 protein in a low pH elution buffer under flow at two different temperatures. ATR-FTIR spectroscopic imaging has several advantages over other commonly used analytical tools for quantification and characterisation of protein aggregates, such as size exclusion chromatography (SEC), dynamic light scattering (DLS) and circular dichroism (CD). This technique yields information on the secondary structure of any aggregates formed, whereas SEC and DLS only provide information on the quantity and size of aggregates. In addition, ATR-FTIR spectroscopic imaging can be applied to high concentration, viscous or turbid samples, presenting an advantage when studying aggregate formation, where protein may precipitate out of solution.[23–26] In addition, analysis of samples taken directly from the bioprocess is possible without the need for dilution steps or sample preparation. Furthermore, the combination of ATR-FTIR spectroscopic imaging with a microfluidic flow set-up allows for study of IgG under flow, more closely resembling bioprocessing conditions and presenting an opportunity for the method to be coupled to a bioprocessing unit operation. Finally, in a microfluidic set-up, the protein can be subjected to stress conditions (*e.g.* elevated temperature) and spectroscopic data can be collected as aggregation proceeds, capturing the structural changes associated with the protein aggregation process over time.

Here, the IgG4 protein in the low pH buffer was flowed through a microfluidic channel which was heated to 30 °C or 45 °C. Analysis of the resulting chemical images and spectra allowed us to measure both the increase in precipitated protein near the IRE surface (*i.e.* the increase in Amide II absorbance) and changes in secondary structure associated with aggregation (*i.e.* shifts in the wavenumber of the Amide I peak position) as a result of exposure to low pH and elevated temperature.

2. Experimental section

2.1. Sample preparation

IgG samples at low pH were prepared in two ways: (1) by collecting the eluted sample directly from the protein A column during purification and (2) through dialysis into 0.1 M sodium citrate (pH 3.5) after the purification process was completed.

Immunoglobulin G monoclonal antibodies were purified from Chinese Hamster Ovary (CHO) cell culture supernatant provided by Prof. Cleo Kontoravdi's lab as described previously.[12,27,28] In brief, frozen supernatant samples were thawed overnight at 4 °C, and the samples were centrifuged for 10 minutes at 3000*g* and filtered using a 0.45 μm disk filter. Low molecular weight contaminants and salts were removed by three cycles through a HiPrep desalting column (GE Healthcare) with the protein eluting into 50 mM phosphate containing 150 mM NaCl, pH 7.4. The collected material was loaded onto a 4.7 ml HiScreen MabSelect PrismA column (Cytiva). After a wash step with phosphate buffer, pH 7.4, IgG was eluted from the column using 0.1 M sodium citrate, pH 3.5. For the IgG samples that were studied directly after elution, the purification process stopped here. The concentration of each 300 μl fraction was measured using a NanoDrop Lite spectrophotometer (Thermo Scientific), and an estimate of the pH was made using pH test strips. After this, selected fractions were used for measurements in an ATR-FTIR spectroscopic imaging flow set-up.

For the samples studied after dialysis, the purification process was completed. In this case, the eluted protein was collected in a collection tube containing 1 M Tris–HCl, pH 9.0 in a 1 : 5 v/v ratio of buffer to eluted protein and each fraction was directly put on ice after collection. As a final purification and buffer exchange step, the pooled fractions were applied to a HiLoad® 16/600 Superdex® 200 pg column (Cytiva) pre-equilibrated with 50 mM phosphate containing 150 mM NaCl, pH 7.4. The resulting IgG fractions were combined and concentrated to 5 mg ml^{-1}. The sample was then divided into aliquots, snap-frozen using liquid N_2 and stored at −70 °C until further use. For each flow experiment analysing IgG at low pH, a fresh aliquot of 5 mg ml^{-1} IgG in phosphate buffer, pH 7.4 was thawed on ice and dialysed into 0.1 M sodium citrate at pH 3.5. Dialysis was performed overnight at 4 °C using cellulose BioDesign™ dialysis tubing (Thermo Fisher Scientific) with a molecular weight cut-off of 14 kDa. The sample was then concentrated to 10 mg ml^{-1} using a 50 kDa molecular weight cut-off filter (Thermo Fisher Scientific). For the control flow experiments where IgG in phosphate buffer was analysed, aliquots were thawed and directly concentrated to 10 mg ml^{-1}.

2.2. ATR-FTIR spectroscopic imaging

Spectroscopic imaging measurements were performed using a Tensor 27 spectrometer (Bruker Corp.) coupled to an IMAC large sample compartment. The Golden Gate accessory (Specac Ltd, UK), with a diamond internal reflection element (IRE) and a 45° angle of incidence, was selected as the most suitable accessory for flow experiments, as the diamond crystal is compatible with low pH samples. The Golden Gate heat controller (Specac Ltd, UK) was used to heat the diamond rapidly to the desired temperatures. Using an MCT focal plane array (FPA) detector with 64 × 64 pixels, 4096 spectra could be collected simultaneously. Measurements were taken in continuous scan mode over the range 900–3900 cm^{-1}, co-adding 32 scans at a spectral resolution of 4 cm^{-1}. Since the imaging view of the Golden Gate accessory is ~0.6 mm (vertical) × 0.55 mm (horizontal),[29] a PDMS flow channel of dimensions 16 mm × 0.5 mm × 0.5 mm was fabricated such that the whole channel could fit within the imaging view. The anvil of the Golden Gate accessory was used to secure the flow channel with a PMMA top plate (inlet and outlet) onto the diamond crystal. It should be noted that the channel width decreases when it is pressed onto the crystal, due to the elasticity of the PDMS material. The inlet of the channel was connected to a 1 ml syringe through PTFE tubing of 0.5 mm inner diameter; the outlet of the channel was connected to a waste vial using the same tubing material. A constant flow of 2.5 μl min^{-1} through the channel was controlled using a syringe pump (Harvard Apparatus). A schematic overview of the set-up can be found in Fig. S1.

2.3. Experimental procedure

For both sets of IgG samples at low pH, flow experiments were carried out at two temperatures, 30 °C and 45 °C. Each flow experiment started with a measurement of the buffer flowing through the channel at room temperature (*i.e.* sodium citrate buffer at pH 3.5 or phosphate buffer at pH 7.4). Then, the IgG sample was flowed through at 2.5 μl min^{-1} and measurements were taken at room temperature and after heating for 0 to 30 minutes at 3 minute intervals. The t = 0 measurement was taken as soon as the desired temperature was reached.

2.4. Data analysis

The integrated absorbance of the Amide I band (1700–1600 cm^{-1}) was plotted for each measurement to generate chemical images, and average spectra were subsequently extracted from the middle of the channel. Buffer subtraction was performed on each spectrum using OPUS (Bruker Corp.) and the resulting Amide I and Amide II bands were used for structural analysis and protein quantification, respectively. Second derivative spectra of the Amide I band were generated in OPUS using 13-point Savitzky–Golay smoothing, unless stated otherwise. Further analysis, including baseline subtraction, was done using OriginPro (OriginLab, Northampton, MA).

3. Results and discussion

3.1. IgG in a low pH elution buffer prepared through dialysis

The results of the 30 °C flow experiments, using IgG that had been dialysed back into a low pH elution buffer after purification and storage, are shown in Fig. 1. Spectroscopic images, generated by integrating over the Amide I band (1700–1600 cm^{-1}), show high absorbance for the protein solution flowing through the channel and low absorbance for the PDMS channel material. The black boxes in Fig. 1A indicate the areas within the channel from which an average spectrum was extracted for each time point. A slight change in absorbance can be observed in the spectroscopic images between the room temperature measurement and the measurements

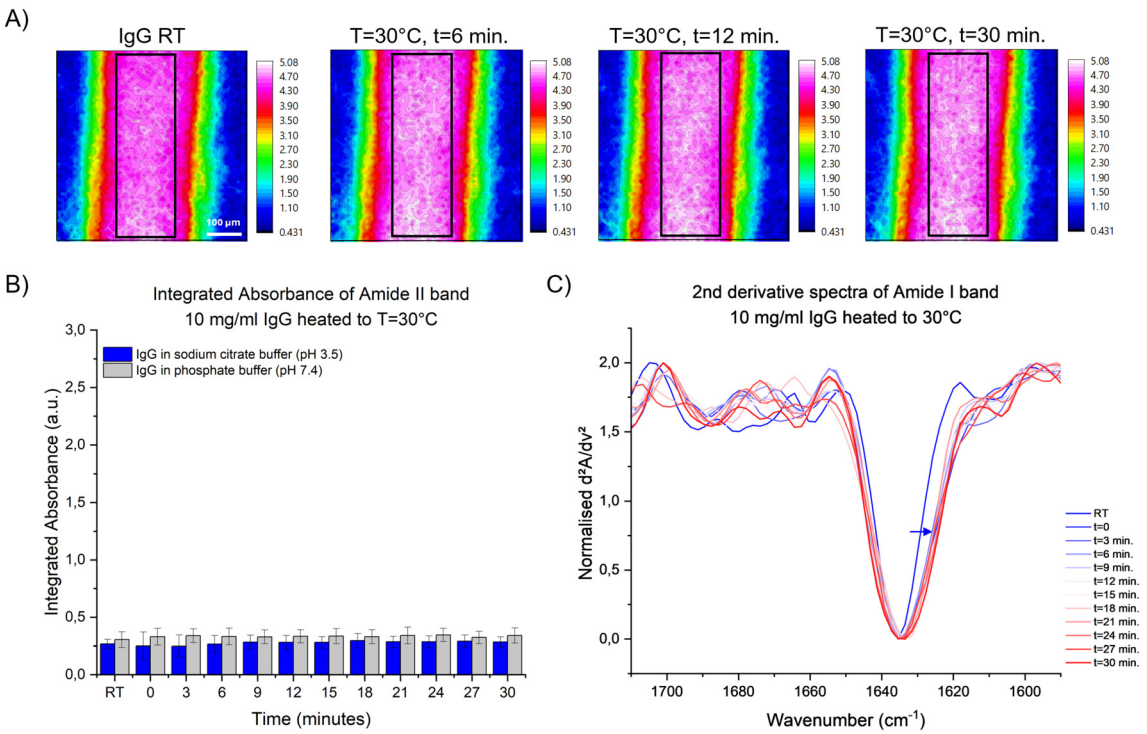

Fig. 1 Flow experiments of 10 mg ml^{-1} IgG in sodium citrate buffer (pH 3.5) *versus* phosphate buffer (pH 7.4) at T = 30 °C. (A) Chemical images of the flow channel generated by Amide I band integration (1700–1600 cm^{-1}), with the black box indicating the area of the spectral extraction. (B) Integrated Amide II absorbance (1580–1490 cm^{-1}) after buffer subtraction (n = 3). Error bars indicate the standard deviation. (C) Second derivative spectra of IgG in 0.1 M sodium citrate buffer (pH 3.5) at room temperature (RT) and after t = 0–30 minutes of heating at T = 30 °C.

taken between t = 0 and t = 30 minutes of heating; however, quantification of the amount of protein was achieved through integration over the Amide II band (1580–1490 cm^{-1}). Quantification of the protein near the IRE surface was based on the Amide II band rather than the Amide I band, as the latter overlaps with the water bending mode (~1640 cm^{-1}). Fig. 1B shows the integrated Amide II absorbance over time for IgG in the sodium citrate buffer during the T = 30 °C flow experiments, with the results obtained from IgG in phosphate buffer as a control. These data show no significant difference in Amide II absorbance between the two buffer conditions at T = 30 °C. However, when comparing the normalised second derivative spectra of IgG in the sodium citrate buffer (Fig. 1C), a clear difference can be observed between the room temperature measurement and the measurements taken after t = 0 to t = 30 minutes of heating. In addition to a peak shift from 1636 cm^{-1} to 1633 cm^{-1}, peak broadening can be observed towards the lower wavenumber region, suggesting the presence of a small population of structurally changed IgG molecules.[30,31] In the control experiment with 10 mg ml^{-1} IgG in phosphate buffer (pH 7.4), minimal changes in the Amide I band were observed (Fig. S2), in line with expectations of IgG stability at neutral pH exposed to 30 °C for a short period of time.

Following the 30 °C flow experiment, the same set-up was used to investigate the mAb stability at 45 °C. This temperature represents an extreme condition, rather than a typical temperature encountered during bioprocessing. Nonetheless, exposure to an extreme condition over a short period of time (*e.g.* heating to 45 °C for 30 minutes) may be useful as a proxy for prolonged exposure (*e.g.* room temperature for several hours). Indeed, the mAbs eluting from the protein A column may be held in the low pH buffer for anywhere between 30 minutes up to several hours as part of the viral inactivation process and the process is typically carried out at temperatures >15 °C.[16,17]

Fig. 2 presents the results of the 45 °C flow experiments, where Fig. 2A and B show the spectroscopic images and average spectra of one of the three repeat experiments with IgG in sodium citrate (pH 3.5). Just from the chemical images, a clear difference can be observed in the absorbance of the Amide I band over the different time points. This increase in absorbance is reflected in the average spectra that were extracted from the channel at each time point (Fig. 2B). The Amide I and Amide II bands both show a steep increase in absorbance, demonstrating the increase of protein near the surface of the IRE. Finally, Fig. 2C shows the integrated Amide II absorbance for IgG in sodium citrate buffer and phosphate buffer during the T = 45 °C flow experiments (n = 3). Unlike during the T = 30 °C experiments, we observe a steady increase in Amide II absorbance over time for IgG in the low pH buffer, suggesting buildup of protein near the surface of the IRE, likely due to the irreversible formation and precipitation of

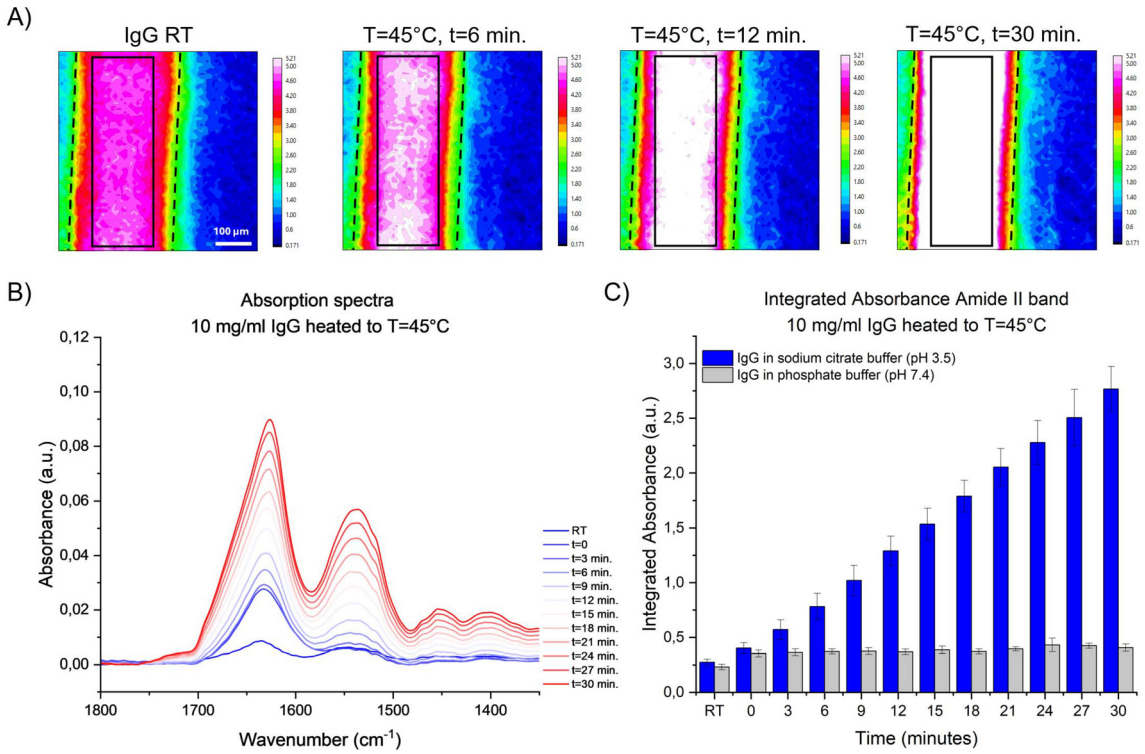

Fig. 2 Flow experiments of 10 mg ml^{-1} IgG in sodium citrate buffer (pH 3.5) *versus* phosphate buffer (pH 7.4) at T = 45 °C. (A) Chemical images of the flow channel generated through Amide I band integration (1700–1600 cm^{-1}), with the black box indicating the area of spectral extraction and the dashed lines indicating the channel wall. (B) Buffer-subtracted spectra of IgG in 0.1 M sodium citrate buffer extracted from the flow channel. (C) Integrated Amide II absorbance (1580–1490 cm^{-1}) after buffer subtraction (n = 3). Error bars indicate the standard deviation.

aggregates. For the control sample, only a small increase in Amide II absorbance is observed between room temperature and t = 0 of heating, and no further increase is detected for the following time points.

We observed small changes in the normalised second derivative spectra of the Amide I band upon heating to 30 °C, specifically the broadening of the main peak towards the lower wavenumber region. Exposure to the higher temperature has a much larger effect on the structural stability of IgG (Fig. 3). The main peak in the second derivative spectrum has moved from 1635 cm^{-1} (predominantly intra-molecular beta sheets) to 1624 cm^{-1} (inter-molecular beta sheets) (Fig. 4A).[28,30,32] This large shift in the peak position is likely due to the unfolding of the native IgG structure, followed by the formation of aggregates.[13] By plotting the normalised absorbance of the two relevant wavenumbers – 1635 cm^{-1} representing native IgG and 1624 cm^{-1} representing aggregated IgG – the structural change over time can be quantified (Fig. 3B). For IgG in phosphate buffer at pH 7.4, the second derivative spectra showed a small shift in the main peak from 1636 cm^{-1} to 1634 cm^{-1}, in addition to broadening of the peak to a lower wavenumber region (Fig. S2).

Based on these results, it can be concluded that IgG in sodium citrate buffer (pH 3.5) is much more prone to aggregation than IgG in phosphate buffer (pH 7.4), in line with previous studies.[13,18] The deleterious effects of the low pH environment on IgG are magnified during heating for 30 minutes, and this gives an indication of what might happen upon a several hour low pH hold following protein A chromatography. The results presented here suggest that the melting temperature of IgG in the low pH environment has significantly dropped compared to IgG in the neutral pH environment. IgG in phosphate buffer at pH 7.4 shows minimal signs of aggregation when heated to 45 °C during the flow experiments, while IgG in elution buffer at pH 3.5 undergoes significant structural changes and precipitates at the channel surface. This is in agreement with a previous study by Ejima *et al.*, which investigated the melting temperature of a humanised IgG4 mAb under acidic conditions using differential scanning calorimetry (DSC). In this case, the native IgG4 sample in phosphate buffer (pH 6.0) exhibited a major endothermic peak at 78 °C and a minor peak at 67 °C; however, these peaks shifted to 58 °C and 35 °C, respectively, for the same protein in a low pH elution buffer (pH 3.5).[21] Furthermore, Jin *et al.* measured the melting temperature of an IgG4-N1 mAb over a range of pH values (pH 3.3–pH 9.0) using differential scanning fluorimetry (DSF) and found that the protein's melting temperature dropped from 67 °C at pH 7.0 to 39 °C at pH 3.6.[16] Additional data using a ZnSe IRE obtained from our lab show that 10 mg ml^{-1} IgG in phosphate buffer (pH 7.4) only starts aggregating from temperatures >60 °C (Fig. S3), comparable to results obtained using a DLS

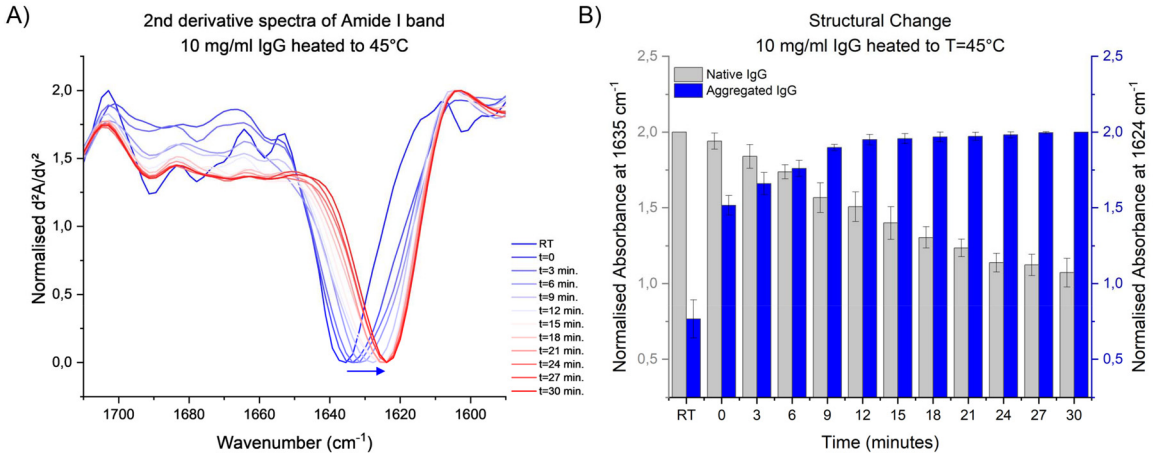

Fig. 3 Change in the secondary structure of 10 mg ml^{-1} IgG in sodium citrate buffer (pH 3.5) during 45 °C flow experiments. (A) Normalised second derivative spectra of the Amide I band during the T = 45 °C flow experiment, clearly showing a shift in peak position from 1635 cm^{-1} (intra-molecular beta sheets) to 1624 cm^{-1} (inter-molecular beta sheets). (B) Normalised absorbance of second derivative spectra at 1635 cm^{-1} and 1624 cm^{-1} over time (n = 3). Note that the values plotted in this figure were obtained by flipping the second derivative spectra of (A) around the x-axis and offsetting the spectra by a value of 2. Error bars indicate the standard deviation.

temperature ramp study and reported melting temperatures of IgG mAbs in the literature.[32–34]

3.2. IgG directly eluted from the column

The results described in section 3.1 provided sufficient confidence in the applicability and reproducibility of ATR-FTIR spectroscopic imaging to study IgG subsequently after eluting from the protein A column. The IgG samples studied in section 3.1 were prepared through overnight dialysis of previously purified IgG into a low pH elution buffer, followed by centrifugation to reach a concentration of 10 mg ml^{-1}. This does not fully represent the conditions of the low pH elution during protein A chromatography and the subsequent low pH hold of a typical bioprocess. Therefore, we also studied IgG samples directly eluted from the protein A column, as this more closely resembles the conditions under which the protein would be found during bioprocessing.

Three individual purifications were completed to obtain three IgG samples, each with a different concentration after fraction collection (*i.e.* 13.6 mg ml^{-1}, 19.5 mg ml^{-1} and 22.2 mg ml^{-1}). The range of concentrations was a result of the starting concentration of IgG in the supernatant, as each of the supernatant samples was produced from a different fed-batch cell culture. Fig. S4 presents the IgG concentration and pH of each of the collected fractions of purifications 1–3. In order to obtain sufficient material for the flow experiments, three 300 µl fractions were selected and combined after the elution was completed. This selection was based on the pH and concentration (*i.e.* highest combined concentration possible where the solution pH of each fraction reached pH 3.5).

Flow experiments were conducted at 30 °C and 45 °C for each of the IgG samples, starting with the lower temperature (*i.e.* half of the protein sample was used for the 30 °C flow experiment, while the other half was kept on ice until the start of the 45 °C flow experiment, roughly 3 hours later). The same trends were found for these samples as those observed for the IgG samples prepared through dialysis (Fig. 4). That is, (i) the Amide II absorbance increases slightly between the RT measurement and the first time point of heating at 30 °C; (ii) the Amide II absorbance remains stable between time points t = 0 and t = 30 minutes of heating to 30 °C (Fig. 4A); and (iii) small changes in the second derivative of the Amide I band can be observed, indicating changes in secondary structure of at least part of the IgG population near the IRE upon heating (Fig. 4B). The three different IgG concentrations behaved similarly, as can be seen in Fig. 4 and Fig. S5. As expected, the Amide II absorbance of the 13.6 mg ml^{-1} sample resulting from purification 1 is measurably smaller than those of the 19.5 mg ml^{-1} and 22.2 mg ml^{-1} samples resulting from purifications 2 and 3, respectively (Fig. 4A).

Following the 30 °C flow experiment, the remainder of the IgG sample, which was stored on ice while the first flow experiment proceeded, was used for the 45 °C flow experiment. As before, the results are in line with those obtained from the protein samples prepared through dialysis. Fig. 5A presents the steep increase in Amide II absorbance upon heating to 45 °C for all three concentrations; Fig. 5B shows the shift in Amide I peak position for the highest concentration mAb sample. Interestingly, the 19.5 mg ml^{-1} sample (purification 2) seems to aggregate at a higher rate than the 22.2 mg ml^{-1}, based on the slope of the Amide II absorbance increase over time. The 13.6 mg ml^{-1} sample (purification 1) and the 22.2 mg ml^{-1} sample (purification 3), although differing substantially in concentration, resulted in comparable slopes (*i.e.* integrated Amide II absorbance over time). This suggests that a higher IgG concentration does not necessarily result in a higher rate of aggregation, indicating that there must be (an) other factor(s) at play. One possible explanation for this differ-

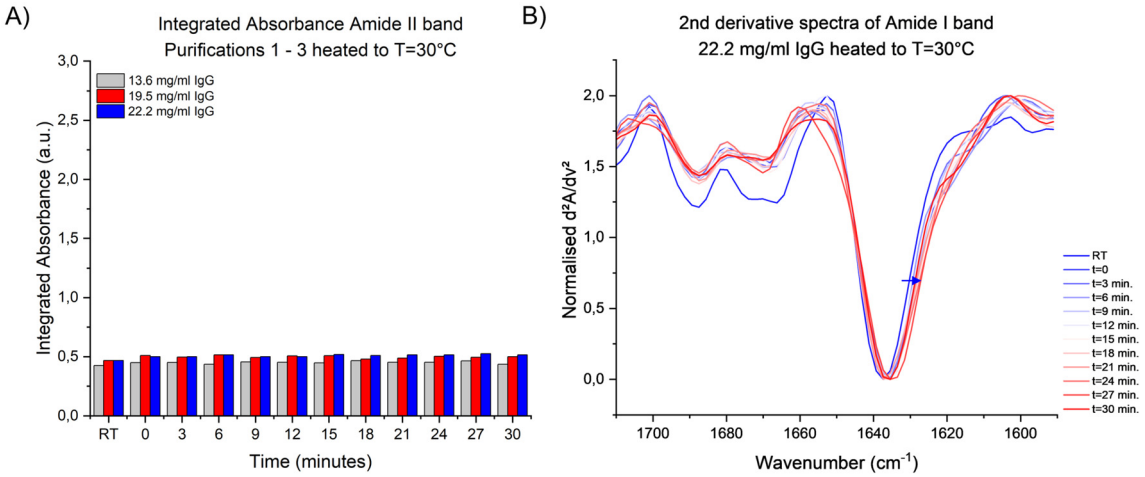

Fig. 4 Results of T = 30 °C flow experiments with IgG in 0.1 M sodium citrate (pH 3.5) after elution from the protein A column. (A) Integrated Amide II absorbance (1580–1490 cm^{-1}) after buffer subtraction for samples from purifications 1–3. (B) Second derivative spectra of the IgG sample obtained from purification 3 (22.2 mg ml^{-1}) at room temperature (RT) and after t = 0 and t = 30 minutes of heating to T = 30 °C.

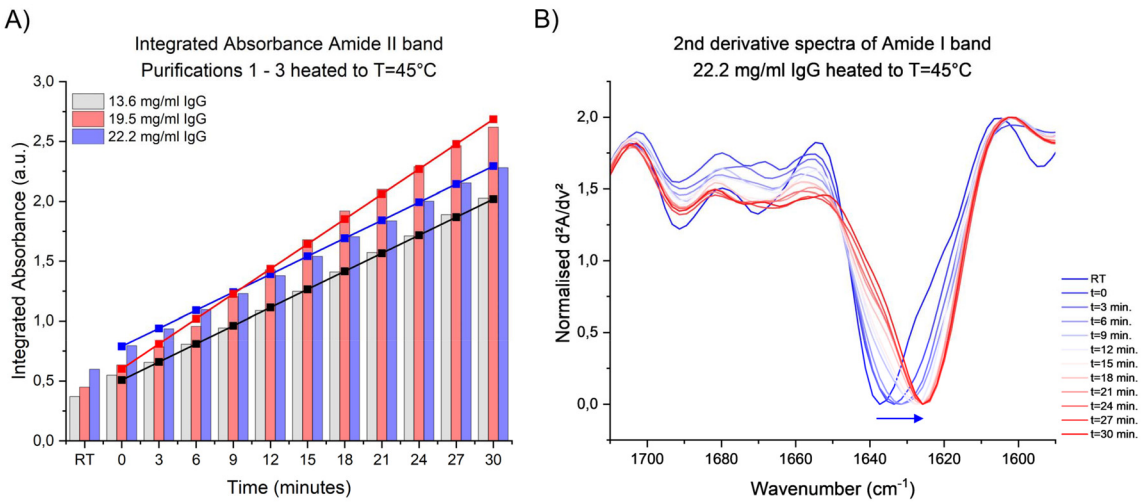

Fig. 5 Results of T = 45 °C flow experiments with IgG in 0.1 M sodium citrate (pH 3.5) after elution from the protein A column. (A) Integrated Amide II absorbance (1580–1490 cm^{-1}) after buffer subtraction for samples from purifications 1–3. (B) Second derivative spectra of the IgG sample obtained from purification 3 (22.2 mg ml^{-1}) at room temperature (RT) and after t = 0 to t = 30 minutes of heating to T = 45 °C.

ence can be found based on the SEC traces of the pooled leftover sample of purifications 2 and 3 (Fig. S6). These SEC samples consisted of all the collected fractions that were not used for the flow experiments, pooled and combined with Tris buffer (pH 9.0). The SEC step was performed the day after protein A purification and the associated flow experiments. Fig. S6 clearly shows an aggregation peak for the SEC trace of purification 2; however, no such peak is present in the SEC trace of purification 3. This could be an indication that the sample of purification 2 used for the flow experiments (19.5 mg ml^{-1} sample) may have contained a small amount of aggregates, leading to a higher Amide II absorbance increase over time compared to the sample of purification 3 (22.2 mg ml^{-1} sample). Although it is unclear why purification 2 contained a small amount of aggregates after protein A chromatography, this variability in IgG samples was reflected in the results of the heated flow experiments, demonstrating the method's applicability to protein stability testing.

Another observation is the change in the second derivative spectrum of IgG measured at room temperature prior to the T = 30 °C and T = 45 °C flow experiments. There is a change in the lower wavenumber region between the first RT measurement and the second RT measurement about 3 hours later, suggesting a change in the secondary structure of the protein. This phenomenon was consistent between the three purifications, although more profound in the higher concentration samples (Fig. S7). In a simple control experiment, we prepared 10 mg ml^{-1} and 20 mg ml^{-1} IgG in sodium citrate (pH 3.5)

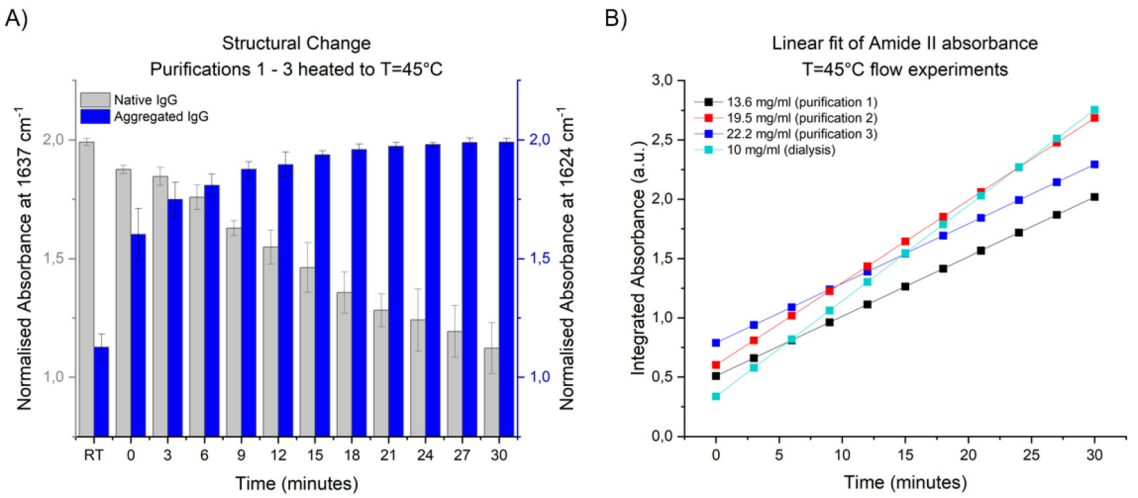

Fig. 6 Structural change based on the Amide I band. (A) Normalised absorbance of second derivative spectra at 1637 cm^{-1} and 1624 cm^{-1} over time (purifications 1–3). Error bars indicate the standard deviation. (B) Comparison of linear fits of Amide II absorbance over time of IgG prepared through dialysis (cyan) *versus* IgG obtained directly after protein A chromatography (black, red, blue).

through dialysis and measured the absorption spectrum every hour for a period of 8 hours while keeping the sample on ice. For the t = 0 measurement, the Amide I band shows a main peak at 1637 cm^{-1}, representing predominantly the native IgG structure, and for the time points thereafter, no significant spectral changes are observed (Fig. S8). These results suggest that IgG in the low pH elution buffer can be stored on ice for at least up to 8 hours without undergoing secondary structural changes, which is in agreement with previously reported studies.[13,21] Since these control samples were prepared through dialysis, they may not behave the same as the samples prepared in purifications 1–3, which were collected directly from the column. However, the change in secondary structure between the two room temperature measurements is likely not solely due to the storage on ice. One other possible factor that may have played a role is the cleaning and reuse of the PDMS channel between the two flow experiments.

Nonetheless, the structural changes observed in the second derivative spectra seem to have a limited effect on the degree of aggregation. This can be concluded from the comparison of the Amide II integrated absorbance graphs of the dialysis-prepared samples *versus* the samples obtained directly after elution (Fig. 6B). From the changed secondary structure of IgG at room temperature, one would expect a relatively high aggregation rate for the protein heated to 45 °C. However, the dialysis-prepared samples of 10 mg ml^{-1} IgG, which show a mostly native secondary structure profile at room temperature, exhibit a significantly higher aggregation rate. The most probable explanation for the relatively low stability of these samples is the preparation method: (i) overnight dialysis includes prolonged exposure to acidic conditions, as well as exposure to the dialysis membrane and (ii) concentration through multiple rounds of centrifugation. Interestingly, when comparing the normalised structural changes over time between the two sample preparation methods, we observe highly similar profiles (Fig. 3B and 6A).

4. Conclusion

ATR-FTIR spectroscopic imaging in combination with microfluidics has proved to be a useful method for the study of protein solutions[28,35] and was employed in this study to assess the structural stability of IgG in a low pH elution buffer. The results presented here confirm that IgG in the low pH elution buffer (pH 3.5) is much less stable than IgG in phosphate buffer (pH 7.4), and this effect is exacerbated by exposure to elevated temperatures.

IgG samples in elution buffers were prepared through (i) dialysis and (ii) elution directly from the protein A column. The overall trends found for both samples were similar, with only small structural changes detected during 30 °C heating and rapid aggregate formation during 45 °C heating. Interestingly, the samples obtained directly after elution seemed more stable, based on the slower increase in Amide II absorbance over time for all three concentrations tested, compared to the 10 mg ml^{-1} IgG sample prepared through dialysis.

Previous work by our group has demonstrated the potential of using ATR-FTIR spectroscopic imaging as an *in situ* measurement technique during protein A chromatography, with a focus on protein A resin fouling and the effect of cleaning-in-place on the column.[12,36,37] In this work, we focused on the stability of the IgG eluate obtained after protein A chromatography. The fabrication of a microfluidic channel for the Golden Gate accessory allowed for measurement of IgG formulations at low pH under flow, while heating at the same time. This set-up can easily be adapted to cater to the study of

various conditions that may be of interest to formulation scientists, as well as providing an in-line measurement technique in conjunction with other bioprocessing operations, not limited to protein A chromatography. Future work may be focused on the development of more sophisticated channel designs, including multiple channels, making in-line measurements possible.

Conflicts of interest

There are no conflicts to declare.

Data availability

Data for this article, including Excel files containing processed spectra, absorbance data and purification data, are available on Figshare at **https://doi.org/10.6084/m9.figshare.29370368**.

Additional figures supporting this article have been included as part of the Supplementary information. See DOI: **https://doi.org/10.1039/d5an00664c**.

Acknowledgements

C. v. H. was funded by the Marit Mohn PhD studentship at the Department of Chemical Engineering.

References

1 G. Walsh and E. Walsh, Biopharmaceutical benchmarks 2022, *Nat. Biotechnol.*, 2022, **40**(12), 1722–1760.
2 R. M. Lu, Y. C. Hwang, *et al.*, Development of therapeutic antibodies for the treatment of diseases, *J. Biomed. Sci.*, 2020, **27**, 1.
3 H. Tiernan, B. Byrne and S. G. Kazarian, ATR-FTIR spectroscopy and spectroscopic imaging for the analysis of biopharmaceuticals, *Spectrochim. Acta, Part A*, 2020, **241**, 118636.
4 B. Kelley, The history and potential future of monoclonal antibody therapeutics development and manufacturing in four eras, *mAbs*, 2024, **16**(1), 2373330.
5 K. Sheehan, H. Jeon, *et al.*, Antibody Aggregation: A problem within the biopharmaceutical industry and its role in AL amyloidosis disease, *Protein J.*, 2025, **44**(1), 1–20.
6 A. J. Paul, K. Schwab and F. Hesse, Direct analysis of mAb aggregates in mammalian cell culture supernatant, *BMC Biotechnol.*, 2014, **14**, 99.
7 T. K. Das, D. K. Chou, *et al.*, Nucleation in protein aggregation in biotherapeutic development: A look into the heart of the event, *J. Pharm. Sci.*, 2022, **111**(4), 951–959.
8 M. E. Krause and E. Sahin, Chemical and physical instabilities in manufacturing and storage of therapeutic proteins, *Curr. Opin. Biotechnol.*, 2019, **60**, 159–167.
9 M. Shah, Commentary: New perspectives on protein aggregation during Biopharmaceutical development, *Int. J. Pharm.*, 2018, **552**(1–2), 1–6.
10 A. R. Mazzer, X. Perraud, *et al.*, Protein A chromatography increases monoclonal antibody aggregation rate during subsequent low pH virus inactivation hold, *J. Chromatogr., A*, 2015, **1415**, 83–90.
11 A. A. Shukla, P. Gupta and X. Han, Protein aggregation kinetics during Protein A chromatography: case study for an Fc fusion protein, *J. Chromatogr., A*, 2007, **1171**(1–2), 22–28.
12 J. W. Beattie, R. C. Rowland-Jones, *et al.*, Insight into purification of monoclonal antibodies in industrial columns studies of Protein A binding capacity by ATR-FTIR spectroscopy, *Analyst*, 2021, **146**(16), 5177–5185.
13 A. Singla, R. Bansal, *et al.*, Aggregation kinetics for IgG1-based monoclonal antibody therapeutics, *AAPS J.*, 2016, **18**(3), 689–702.
14 J. W. Beattie, A. Istrate, *et al.*, Causes of industrial Protein A column degradation, explored using Raman spectroscopy, *Anal. Chem.*, 2022, **94**(45), 15703–15710.
15 P. Gagnon, R. Nian, *et al.*, Transient conformational modification of immunoglobulin G during purification by protein A affinity chromatography, *J. Chromatogr., A*, 2015, **1395**, 136–142.
16 W. X. Jin, Z. Z. Xing, *et al.*, Protein aggregation and mitigation strategy in low pH viral inactivation for monoclonal antibody purification, *mAbs*, 2019, **11**(8), 1479–1491.
17 R. Wälchli, M. Ressurreiçao, *et al.*, Understanding mAb aggregation during low pH viral inactivation and subsequent neutralization, *Biotechnol. Bioeng.*, 2020, **117**(3), 687–700.
18 E. Y. Chi, S. Krishnan, *et al.*, Physical stability of proteins in aqueous solution: Mechanism and driving forces in nonnative protein aggregation, *Pharm. Res.*, 2003, **20**(9), 1325–1336.
19 F. Bickel, E. M. Herold, *et al.*, Reversible NaCl-induced aggregation of a monoclonal antibody at low pH: Characterization of aggregates and factors affecting aggregation, *Eur. J. Pharm. Biopharm.*, 2016, **107**, 310–320.
20 P. Arosio, S. Rima and M. Morbidelli, Aggregation mechanism of an IgG2 and two IgG1 monoclonal antibodies at low pH: From oligomers to larger aggregates, *Pharm. Res.*, 2013, **30**(3), 641–654.
21 D. Ejima, K. Tsumoto, *et al.*, Effects of acid exposure on the conformation, stability, and aggregation of monoclonal antibodies, *Proteins*, 2007, **66**(4), 954–962.
22 H. Fukada, K. Tsumoto, *et al.*, Long-term stability and reversible thermal unfolding of antibody structure at low pH: Case study, *J. Pharm. Sci.*, 2018, **107**(11), 2965–2967.
23 H. Y. Yang, S. N. Yang, *et al.*, Obtaining information about protein secondary structures in aqueous solution using Fourier transform IR spectroscopy, *Nat. Protoc.*, 2015, **10**(3), 382–396.
24 N. J. Greenfield, Using circular dichroism spectra to estimate protein secondary structure, *Nat. Protoc.*, 2006, **1**(6), 2876–2890.

25 J. Stetefeld, S. A. McKenna and T. R. Patel, Dynamic light scattering: a practical guide and applications in biomedical sciences, *Biophys. Rev.*, 2016, **8**(4), 409–427.
26 R. R. Burgess, A brief practical review of size exclusion chromatography: Rules of thumb, limitations, and troubleshooting, *Protein Expression Purif.*, 2018, **150**, 81–85.
27 H. Tiernan, B. Byrne and S. G. Kazarian, Insight into heterogeneous distribution of protein aggregates at the surface layer using attenuated total reflection-Fourier transform infrared spectroscopic imaging, *Anal. Chem.*, 2020, **92**(7), 4760–4764.
28 C. van Haaren, B. Byrne and S. G. Kazarian, Study of monoclonal antibody aggregation at the air-liquid interface under flow by ATR-FTIR spectroscopic imaging, *Langmuir*, 2024, **40**(11), 5858–5868.
29 E. Possenti, C. Colombo, *et al.*, Time-resolved ATR-FTIR spectroscopy and macro ATR-FTIR spectroscopic imaging of inorganic treatments for stone conservation, *Anal. Chem.*, 2021, **93**(44), 14635–14642.
30 S. Matheus, W. Friess and H. C. Mahler, FTIR and nDSC as analytical tools for high-concentration protein formulations, *Pharm. Res.*, 2006, **23**(6), 1350–1363.
31 M. van de Weert, P. I. Haris, *et al.*, Fourier transform infrared spectrometric analysis of protein conformation: Effect of sampling method and stress factors, *Anal. Biochem.*, 2001, **297**(2), 160–169.
32 G. Baird, C. Farrell, *et al.*, FTIR spectroscopy detects intermolecular β-Sheet formation above the high temperature Tm for two monoclonal antibodies, *Protein J.*, 2020, **39**(4), 318–327.
33 T. Ito and K. Tsumoto, Effects of subclass change on the structural stability of chimeric, humanized, and human antibodies under thermal stress, *Protein Sci.*, 2013, **22**(11), 1542–1551.
34 E. Koepf, R. Schroeder, *et al.*, The film tells the story: Physical-chemical characteristics of IgG at the liquid-air interface, *Eur. J. Pharm. Biopharm.*, 2017, **119**, 396–407.
35 H. Tiernan, B. Byrne and S. G. Kazarian, ATR-FTIR spectroscopy and spectroscopic imaging to investigate the behaviour of proteins subjected to freeze-thaw cycles in droplets, wells, and under flow, *Analyst*, 2021, **146**(9), 2902–2909.
36 M. Boulet-Audet, B. Byrne and S. G. Kazarian, Cleaning-in-place of immunoaffinity resins monitored by in situ ATR-FTIR spectroscopy, *Anal. Bioanal. Chem.*, 2015, **407**(23), 7111–7122.
37 M. Boulet-Audet, S. G. Kazarian and B. Byrne, In-column ATR-FTIR spectroscopy to monitor affinity chromatography purification of monoclonal antibodies, *Sci. Rep.*, 2016, **6**, 30526.